Colloids and Surfaces A: Physicochemical and Engineering Aspects 713 (2025) 136486

Contents lists available at ScienceDirect

Colloids and Surfaces A: Physicochemical and Engineering Aspects

journal homepage: www.elsevier.com/locate/colsurfa

Highly efficient boron/sulfur-modified activated biochar for removal of reactive dyes from water: Kinetics, isotherms, thermodynamics, and regeneration studies

Alejandro Grimm [a,*], Sarah Conrad [b], Francesco G. Gentili [a], Jyri-Pekka Mikkola [c,h], Tao Hu [d], Ulla Lassi [d], Luis F.O. Silva [e], Eder Claudio Lima [f,g], Glaydson Simoes dos Reis [h]

[a] Department of Forest Biomaterials and Technology, Biomass Technology Centre, Swedish University of Agricultural Sciences, Umeå SE-901 83, Sweden
[b] Department of Civil, Environmental and Natural Resources Engineering, Luleå University of Technology, Luleå 97187, Sweden
[c] Wallenberg Wood Science Center, Technical Chemistry, Department of Chemistry, Umeå University, Umeå 90187, Sweden
[d] Research Unit of Sustainable Chemistry, University of Oulu, P.O. Box 4300, Oulu FI-90014, Finland
[e] Universidad de La Costa, CUC, Calle 58 # 55–66, Barranquilla, Atlántico, Colombia
[f] Postgraduate Program in Mine, Metallurgical, and Materials Engineering (PPGE3M), School of Engineering, Federal University of Rio Grande do Sul (UFRGS), Av. Bento Gonçalves, Porto Alegre, RS 9500, Brazil
[g] Institute of Chemistry, Federal University of Rio Grande do Sul (UFRGS), Av. Bento Goncalves 9500, Postal Box, 15003, Porto Alegre, RS 91501-970, Brazil
[h] Laboratory of Industrial Chemistry and Reaction Engineering, Faculty of Science and Engineering, Åbo Akademi University, Åbo, Turku 20500, Finland

HIGHLIGHTS

- Pine logging residue was used to produce highly porous boron or sulfur-modified biochars.
- The sample treated with boron showed an exceptional degree of graphitization (I_D/I_G=0.45).
- Reactive Back-5 adsorption capacities (Liu model) were between 1419 and 1766 mg g^{-1}
- Thermodynamic adsorption studies showed that the adsorption process was endothermic.
- B and S-treated biochars kept 60–67 % dye removal capacity after 7 regeneration cycles.

GRAPHICAL ABSTRACT

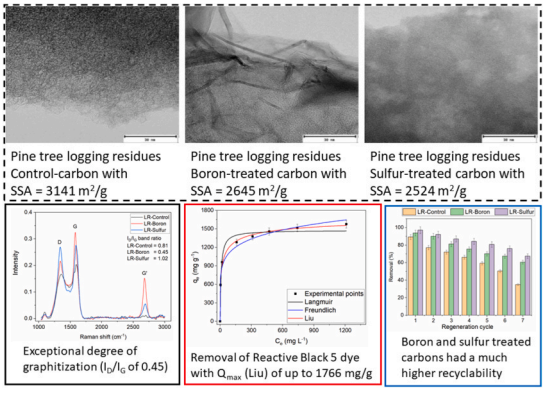

ARTICLE INFO

Keywords:
Logging residues, activated biochar
Boron/sulphur chemical modifiers
Potassium hydroxide activation
Graphitic biochar
Reactive black-5 adsorption
Dye effluents

ABSTRACT

Water pollutants such as synthetic dyes can cause significant problems for human health and ecosystems due to their chemical properties and environmental interactions. Contamination of surface and underground water caused by the discharge of synthetic dyes is a widespread problem that arises primarily from industrial activities such as textile manufacturing, leather processing, paper production, and plastics industries. Since adsorption is one of the most efficient and reliable methods to remove pollutants from water, in this work, pine tree logging residues (LR) were used to produce boron/sulfur chemically modified biochars with superior adsorption

* Corresponding author.
E-mail address: alejandro.grimm@slu.se (A. Grimm).

https://doi.org/10.1016/j.colsurfa.2025.136486
Received 12 November 2024; Received in revised form 14 February 2025; Accepted 20 February 2025
Available online 21 February 2025

performance and recyclability. The biochars were produced using a two-step pyrolysis procedure with potassium hydroxide as a chemical activator. The specific surface areas (B.E.T.) of the biochars were 2645 m^2 g^{-1} for the boron-treated biochar (LR-Boron), 2524 m^2 g^{-1} for the sulfur-treated (LR-Sulfur), and 3141 m^2 g^{-1} for the control biochar (LR-Control, without boron or sulfur), respectively. The LR-Boron biochar showed an exceptional degree of graphitization of (I_D/I_G=0.45), while the LR-Sulfur biochar displayed an I_D/I_G= 1.02; for comparison, the LR-Control exhibited an I_D/I_G= 0.81, showing that the sample subjected to boron treatment created carbon-rich in graphitic structures. The three biochars were evaluated as adsorbents for removing reactive black-5 azo dye (RB-5) from water and mixtures of several dyes in synthetic aqueous effluents. The adsorption data showed that all carbons exhibited outstanding RB-5 removal performance. Kinetic measurements were well fitted by the Avrami fractional order model, and the LR-sulfur carbon displayed the fastest adsorption kinetics. Isotherm measurements were well fitted by the Liu model, with a theoretical Q_{max} of around 1419 mg g^{-1} (LR-Control), 1586 mg g^{-1} (LR-Boron), and 1766 mg g^{-1} (LR-Sulfur) at 316 K. The presence of sulfur-functional groups on the LR-Sulfur biochar surface was probably the reason for the superior adsorption performance of this biochar. Both sulfur and boron-treated biochars exhibited higher regeneration potentials, maintaining around 60–67 % removal capacity after 7 cycles compared to 35 % for the LR-Control biochar. Thermodynamic adsorption studies showed that the adsorption process was endothermic, favorable, and compatible with physical adsorption. All produced biochars were highly efficient for removal of pollutants from concentrated synthetic effluents.

1. Introduction

In recent decades, the issue of water contamination has expanded beyond traditional concerns about pathogens. A growing problem that has emerged is the presence of anthropogenic synthetic pollutants in water used for human consumption, among which, dyes [1,2], pharmaceuticals and personal care products [3,4], bisphenol [5–7], pesticides and herbicides [8,9], hydrocarbons and oil [10,11] and heavy metals [12,13] are the most common. Industries like textile, leather, paper, and plastic are major consumers of water and often use synthetic dyes in their manufacturing processes. If not properly treated before being discharged into the environment, process water contaminated with dyes can cause severe ecological and health problems due to its toxic, carcinogenic, and non-biodegradable nature [14]. The presence of dyes in water also affects its quality and inhibits light penetration, disturbing aquatic life and ecosystems [15].

Conventional methods for dye removal from water, including chemical coagulation, oxidation, membrane filtration, and biological treatments, often face limitations in terms of efficiency, cost, and generation of secondary pollutants [16]. Among various available methods, adsorption has emerged as a highly effective and versatile technique for the removal of dyes from aqueous solutions. Activated biochar, in particular, has been widely recognized as an exceptional adsorbent due to its high surface area, porous structure, and significant adsorption capacity [16–19]. Several factors, including surface properties of the carbon such as specific surface area and functionalization, the type of contaminant, and operational conditions such as pH, temperature, and contact time, determine the efficacy of activated biochar in removing pollutants from water [20].

During the last few years, the concept of heteroatom doping with different elements such as nitrogen [21], selenium [22], sulfur [23], and boron [24], among others, has emerged as a promising and innovative method to enhance the adsorption capacity of traditional activated biochar. Introducing elements such as boron into the carbon matrix imparts unique properties that make it particularly effective in capturing and immobilizing pollutants in water treatment processes [25]. Boron is also a versatile metalloid that significantly enhances the degree of graphitization of activated biochar [26]. The graphitization process involves the transformation of amorphous carbon structures into well-ordered graphite structures, which can substantially improve the material's properties, such as electrical conductivity, π-π interactions, mechanical strength, and electrostatic attractions, among others [27], which in turn may lead to improved adsorption characteristics and endurance against regeneration processes. Using chemical modifiers such as sulfur during the production of activated biochar significantly enhances its adsorption capacity. Sulfur atoms introduce new functional groups, such as C–S, –C–S–C–, C═S, thiophene, and sulfone, onto the surface of the activated biochar [28]. The increased presence of sulfur functional groups enhances the biochar's ability to form strong binding with contaminants, leading to improved adsorption efficiency [29]. The use of sulfur as a chemical modifier also changes the pore structure of activated biochar, as well as its specific surface area, creating a more diverse range of pore sizes that may improve adsorption capacity and mechanical strength [29–31].

According to what was explained above, the use of boron and sulfur during the production of biochar appears promising in terms of improving the adsorption characteristics of regular, non-modified biochars. However, information about the influence of boron and sulfur on the structural and chemical properties of carbon, as well as changes in the adsorption performance and recyclability of spent biochar, is scarce in the literature and not well understood. Thus, this research gives new approaches for the development of efficient carbon materials with improved adsorptive properties for the removal of pollutants from waters. In this work, boron or sulfur-treated activated biochars were produced using logging residues, which include treetops, branches, and other by-products of timber harvesting. In Sweden, Norway, and Finland, logging residues are a good example of an abundant and underutilized resource that could play a crucial role in developing sustainable forestry practices [32]. However, this type of biomass waste is currently used only as fuel in biomass power plants [32–34]. Extending the utilization of logging residues as raw material for the production of activated biochar would help to improve the utilization of this type of biomass residues with a complex composition and a low commercial value. This work shows results from the characterization of chemically modified activated biochars produced using logging residues from pine trees. Boron and sulfur were used as chemical modifiers and potassium hydroxide was used as a chemical activator. The activated biochars were characterized using surface area analysis (BET), X-ray photoelectron spectroscopy (XPS), Raman spectroscopy, scanning electron microscopy (SEM), and high-resolution transmission electron microscopy (HR-TEM). The produced biochars were used to remove Reactive Black-5 dye from water solutions and mixtures of several dyes in synthetic effluents. Kinetic, isotherm, thermodynamic, and regeneration measurements were used to characterize the adsorption process.

2. Materials and methods

2.1. Materials

Logging residues from pine trees (*Pinus sylvestris*) were collected from a clear-felling area in Umeå, Sweden. The material used here was gathered from dried stacks and composed of branches and treetops. The logging residue (approximately 100 kg) was first homogenized using a large-scale hammer mill (Bühler DFZK 1) to a particle size of 20–50 mm.

Next, representative samples (10 kg) were dried in an oven at 105 °C overnight, and then milled using a Retsch SM2000 hammer mill equipped with a 2 mm screen sieve and used for the experiments as is. Elemental boron (> 95 %, Sigma Aldrich) and sulfur powder (99 %, Sigma Aldrich) were used as chemical modifiers, and potassium hydroxide (99.8 %, Supelco) was used as an activator. Reactive black-5 (Sigma Aldrich) was utilized as a model water contaminant in batch adsorption experiments. This dye is a bis(azo) compound belonging to the vinyl sulphone type used extensively in the production of textiles, papers, leathers, plastics, ink, shoe polish, and electroplating among other uses.

2.2. Production of activated boron and sulfur-modified biochars

To maximize the specific surface area of the carbons, a two-step procedure was used to prepare the logging residue-based activated boron (LR-Boron) or sulfur (LR-Sulfur) modified biochar. First, ground logging residue (90 g) was mixed with boron or sulfur (30 g), and water was added to create a homogeneous paste. This mixture was left to soak for 6 hours and dried at 60 °C overnight. After drying, the material was pyrolyzed at 500 °C under a nitrogen gas atmosphere in a stainless-steel reactor inserted in a conventional muffle furnace. The temperature of the sample, monitored with a type N thermocouple, was raised from room temperature (T_R) to the final temperature (T_f) at 5 °C/min and maintained for 1 hour. After this, the furnace was turned off and allowed to cool down to room temperature. Next, the obtained carbon was activated with KOH using a weight ratio of 1:6. The two were mixed, and water (2 mL/g KOH) was added. This mixture was stirred for 6 hours and, after that, dried at 90 °C for 12 h. The resulting material was pyrolyzed at 900 °C, with the reactor temperature increased from T_R to T_f at 5 °C/min and held for 1 hour. After this, the furnace was turned off and allowed to cool down to room temperature. The carbon obtained was washed with water until the pH of the wash water was neutral, and after that, dried at 105 °C overnight to obtain the final product.

For comparison, an activated biochar control sample (LR-Control) was prepared using the same procedure described above but without the chemical modifier.

2.3. Characterisation of activated biochars

Nitrogen adsorption isotherms were measured using a Tristar 3000 device (Micromeritics Instrument Corp., Norcross, GA, USA) and used to determine the specific surface area (SSA) of the biochars produced. The SSA values were obtained based on the Brunauer–Emmett–Teller (B.E.T.) method, while the pore size distribution curves were obtained using the Barrett–Joyner–Halenda (BJH) method. High-resolution transmission electron microscopy (HR-TEM) was used to analyze morphological characteristics and performed by an energy-filtered transmission electron microscope (EFTEM) with scanning transmission electron microscopy (STEM), JEOL JEM-2200FS EFTEM/STEM (JEOL Ltd., Akishima, Tokyo 196–8558, Japan). The sample powders were dispersed in ethanol and pretreated in an ultrasonic bath for several minutes. A small drop of the microemulsion was deposited on a 200 mesh copper grid precoated with carbon (Lacey C, TED PELLA, INC.). The accelerating voltage of the EFTEM/STEM was 200 kV. Raman spectra were collected using an inVia confocal Raman spectroscope (Renishaw) equipped with a 514 nm laser. The surface elemental composition and functionalities were assessed using X-ray photoelectron spectroscopy (XPS) which was performed using a Thermo Fisher Scientific ESCALAB 250Xi XPS System (Thermo Fisher Scientific, 168 Third Avenue, Waltham, MA USA 02451) at the Centre for Material Analysis, University of Oulu (Finland). The powder samples were placed in a gold sample holder. The high-resolution scan used a pass energy of 20 eV while the survey scan used a pass energy of 150 eV. The monochromatic AlKα radiation (1486.7 eV) was operated at 20 mA and 15 kV with an X-ray spot size of 900 μm. Carbon (C), oxygen (O), boron (B), and sulfur (S) were measured in the samples, and the measurement data were analyzed using the Advantage V5 software. Charge compensation was carried out by applying the C1s at 284.8 eV as a reference to determine the presented spectra and calibrate the binding. The point of the zero charge (pH_{pzc}) value of each biochar was obtained by plotting the measured zeta potential value versus pH. Measurements were carried out using a Zetasizer Nano ZSE 3700 (Malvern Instrument Co., UK) at 298 K varying pH from 2 to 10.

2.4. Adsorption experiments

Adsorption experiments of Reactive Black-5 (RB-5) in aqueous solution were conducted in batch mode at pH 6. All experiments were performed using an orbital shaker incubator (Biosan ES-20/80 C) at a constant shaking speed of 300 rpm. The effect of the adsorbent dosage on dye removal was assessed at room temperature (296 K) using dosages ranging from 0.25 to 1 g L^{-1} and a 500 mg L^{-1} RB-5 solution. Kinetic measurements were also conducted at room temperature (296 K), using dye concentrations of 500 mg L^{-1} and 1000 mg L^{-1}, an adsorbent dosage of 0.5 g L^{-1}, and contact times between 0 and 600 minutes. Adsorption isotherms were obtained at temperatures of 296, 306, and 316 K with dye concentrations from 100 to 2000 mg L^{-1} and an adsorbent dosage of 0.5 g L^{-1}. The activated biochars were separated from the solutions by centrifugation at 5000 rpm, and the concentration of RB-5 in the liquid phase was measured using a UV-Vis spectrometer at 597 nm calibrated with standard dye solutions.

The adsorption capacity (q_t and q_e) and percentage of removal (%) were calculated according to the equations given in the supplementary materials. At least three points in each of the measurements were done in triplicate to check for experimental deviations. This was then taken as the standard deviation for all other points.

2.5. Treatment of synthetic effluents

Two aqueous dye-based solutions with different concentrations were made to evaluate the performance of produced biochars to remove contaminants from complex mixtures of water pollutants, here called synthetic effluents. The composition of the tested effluents is shown in Table 1. The adsorption tests were made using adsorbent doses of 0.5 and 1 g L^{-1} at room temperature (296 K). The solutions containing the adsorbents were agitated for 12 h, and after that, the biochar was separated by centrifugation as previously described. The percentage of dye removed from each effluent was calculated based on the integrated area under the UV-Vis spectra (800–190 nm) of each effluent before and after the adsorption process [21].

2.6. Regeneration of spent adsorbents

Biochar samples were saturated with RB-5 solution (C_o = 1000 mg L^{-1}) using the same adsorption methods at 296 K as previously described. After the adsorption first step, the loaded carbon was separated from the solution and washed with deionized water 3 times to remove unadsorbed dye. The loaded carbons were then dried in an oven at 60 °C overnight. The adsorbed dye was then eluted by contacting the

Table 1
Composition of the two synthetic effluents.

Dye	Concentration (mg L^{-1})		λ_{max} (nm)
	Effluent−1	Effluent−2	
Reactive black−5	50	100	597
Reactive red−120	50	100	535
Reactive orange−16	25	50	388 (1st), 494 (2nd)
Reactive blue−4	25	50	595
Methyl red	25	50	410
Crystal violet	25	50	584–590
Evans blue	25	50	605

dye-loaded carbons with 0.2 M NaOH-H_2O in ethanol (30 %). The loaded carbons and eluent were agitated for 6 hours to allow for the dye desorption. The dye and eluent were separated by centrifugation, and the regenerated biochars were washed with deionized water until the wash water achieved a neutral pH and then dried at 60 °C overnight. Seven consecutive adsorption-desorption cycles were done. The percentage of dye removed after each cycle was determined as previously described.

3. Results and discussion

3.1. Textural and surface characteristics

The specific surface area (SSA (S_{BET})) of an adsorbent and the ratio of mesopores to micropores areas are among the most critical features that determine the quality of an adsorbent in terms of its pollutant removal capacity from water. Fig. 1a shows the nitrogen adsorption/desorption isotherms of the carbon materials and the SSA. The pore size distribution of each biochar is shown in Fig. 1b, c and d. The LR-Control biochar shows characteristics of type I isotherms, indicating a carbon matrix with a predominance of microporous structures [35]. For the biochars treated with boron and sulfur, the nitrogen isotherms show characteristics of type IV isotherms, indicating a greater presence of mesopores than in the control sample.

This means that for the carbon precursor used here, using boron or sulfur during the activation process provoked a widening of the pores, which is seen when comparing Fig. 1b (LR-Control) with Fig. 1c (LR-boron) and Fig. 1d (LR-Sulfur) pore size distributions. These differences in pore size could help improve the adsorption performance of pollutants with a large molecular size. The S_{BET} of the LR-Boron (2645 $m^2\ g^{-1}$) and LR-Sulfur (2524 $m^2\ g^{-1}$) biochars was lower than that of the LR-Control biochar (3141 $m^2\ g^{-1}$) due to the higher amount of micropores compared to mesopores in this sample (Fig. 1b).

The impact of the different treatments on the morphological microstructure of the LR-Control, LR-Boron and LR-Sulfur was further examined by SEM (Fig. S1), which shows important differences in their morphologies. LR-Control carbon shows a compact structure with cavities and a huge presence of small pores (Fig. S1b), which matches with the N_2 adsorption isotherm data that showed a huge presence of micropores in LR-Control carbon. LR-Boron presented a more compacted structure with no cavities and a morphology rich in small flakes with high rugosity (Fig. S1c,d). The small flakes could be related to the

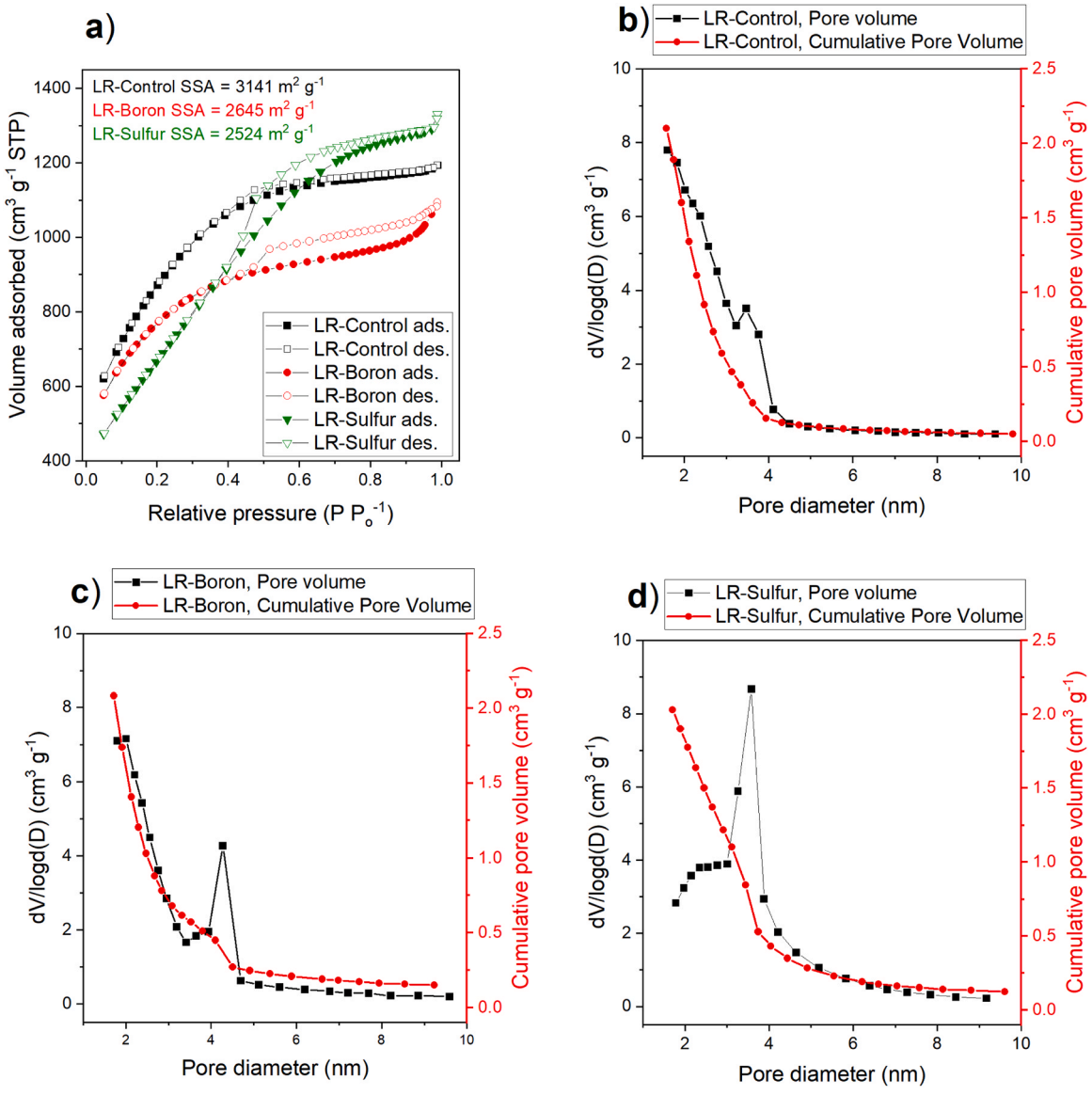

Fig. 1. Nitrogen adsorption-desorption isotherms (77 K) for LR-Control, LR-Boron, and LR-Sulfur activated biochars (a), and pore volume (b, c, d).

graphene-like material (as shown in Raman and HRTEM analysis). LR-Sulfur exhibited remarkable differences in comparison to the others, it displays a very rough surface with a high number of small pores (Fig. S1f). It seems that the incorporation of S enhanced the morphological defects, which may have a positive impact on its ability to adsorb contaminants from polluted waters. However, it is worthwhile to say that all three carbons present different morphologies with great potential for adsorbent applications.

HRTEM analysis was employed to evaluate the effect of the boron and sulfur on the nanostructure of the carbon materials. As can be seen, LR-Control (Fig. 2a) and LR-Sulfur (Fig. 2c) seem to be formed mainly of disordered carbon structures, with no crystalline features being observed. However, the LR-Boron (Fig. 2b) shows a combination of disordered and crystalline structures. A clear presence of graphitized structure and graphene sheets all over its structure reflects a successful graphitization process imposed by the boron treatment. These results align with the literature, which shows that sulfur doping enhances the structural defects in the carbon lattice of carbon materials [29], while boron acts as a catalyst for increasing the graphitization in carbon structures.

The Raman spectra of the produced biochars are shown in Fig. 2d. These spectra are useful to evaluate the amounts of amorphous and crystalline carbon phases and the graphitization degree of the biochars. The D-band is associated with amorphous sp^3- carbon structures, and the G-band shows the amount of crystalline graphitic structures (sp^2) [36, 37]. The Raman spectra of the LR-Boron and LR-Sulfur biochars show the presence of a G' (2D) peak at approximately 2681 cm^{-1}, which is not present in the LR-control biochar [36,37]. The G' peak means that using boron and sulfur as chemical modifiers leads to the formation of carbon structures typical of graphene with a high degree of stacking; however, this formation was much larger when using boron. Boron acts as a catalyst in the graphitization process and, when incorporated into biochar, lowers the activation energy required for the transformation of disordered carbon structures into graphitic domains. This catalytic effect accelerates the rearrangement of carbon atoms, promoting the formation of graphitic layers at lower temperatures (900 °C in this work) than the conventional graphitization process carried out via heating processes at temperatures of around 2500 °C [38,39]. When introduced into the carbon matrix, boron occupies interstitial sites. This interstitial doping facilitates the reorganization of carbon atoms into a more ordered graphitic structure. The presence of boron thus helps to break the stability of amorphous carbon bonds, easing their realignment into graphitic planes.

The I_D/I_G band ratio for each biochar is given in Fig. 2d. A low I_D/I_G ratio indicates the presence of ordered graphitic structures with a high graphitization degree [37]. A higher ratio means that the biochar carbon matrix is richer in defects, meaning there is a higher number of amorphous structures (i.e., increases the number of atoms with sp^3 hybridization). The LR-Boron biochar I_D/I_G ratio (0.45) was the lowest compared to the LR-Sulfur (1.02) and LR-Control (0.81), meaning the biochar produced using sulfur as a chemical modifier has the most disordered carbon matrix compared to the others. This fact is that sulfur is inserted in the carbonaceous matrix, forming C-S, C═S, and C-S-C chemical bonds (see Fig S4, in supplementary materials) contributing to higher disorder as shown in Fig. 2c, and Raman spectra Fig. 2d.

The XPS spectra of the produced biochars are shown in the

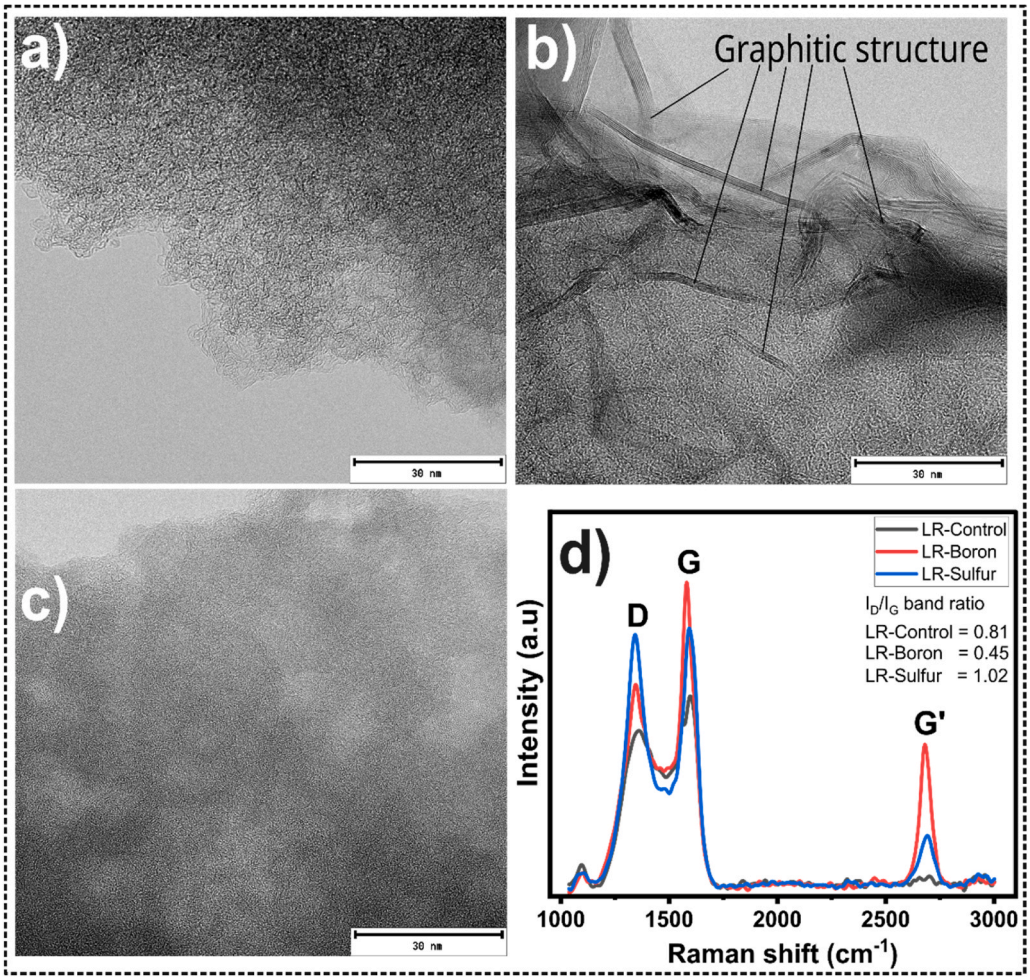

Fig. 2. HRTEM images a) LR-Control, b) LR-Boron, c) LR-Sulfur, and d) Raman Spectra of the produced carbon materials.

supplementary materials Fig. S2, S3, and S4 (supplementary materials), and the surface elemental analysis derived from the spectra is shown in Table 2. The LR-Control and LR-Boron biochars are composed only of carbon and oxygen. Compared to the LR-Control biochar, the LR-Boron sample has a higher content of graphitic carbon (C-C bonds) and transition due to conjugation (π-π) and lower oxygen content, confirming what is seen in the Raman analysis. The C/O ratio of the LR-Boron biochar (53.2 at%) was much higher than that of the LR-Control biochar (32.8 at%). The boron content in the LR-Boron sample is relatively low, which means that boron acted as a graphitization catalyst rather than a dopant. Compared to the control and boron-treated biochar, the LR-Sulfur biochar surface has a lower carbon content and a larger amount of oxygen groups. As shown in Table 2, the sulfur content of this biochar is 5.22 at%, of which 3.3 at% corresponds to sulfides (C-S-C bonds) and 1.92 at% to thiophene (R-S(=O)-R') structures [40].

3.2. Adsorption of reactive black-5

3.2.1. Point of zero charge of the produced activated biochars

The pH_{pzc} plays an important role in understanding the adsorption process. It indicates the pH value in which the adsorbent surface charges are null. It also indicates at which pH the surface of the adsorbent is positively charged (pH below pH_{pzc}) and negatively charged (pH above pH_{pzc}). Comparing the results of the different carbons (see Fig. S5 in Supplementary materials), LR-sulfur exhibited the highest pH_{pzc} value (7.94) followed by LR-Boron (6.52) and LR-Control (4.94), indicating that the sulfur treatment created a more positively charged surface (acid character) at wider pH range. This may have a positive impact on the adsorption process since RB-5 dye has two sulfonate groups and two sulfate-ethyl-sulfone groups, and these groups are negatively charged even in highly acidic solutions due to their pK_a values that are lower than zero [41,42]. Therefore LR-sulfur can easily bind RB-5 through electrostatic interactions.

3.2.2. Adsorbent dosage

The adsorbent dosage is a critical parameter in an activated biochar-based adsorption process, playing a significant role in the efficiency and effectiveness of the contaminant removal, and the rate at which contaminants are adsorbed onto activated biochar. In batch systems, optimizing the adsorbent dosage is essential for economic viability. Overdosing can lead to unnecessary costs without significant gains in adsorption efficiency while using too little can result in poor performance and the need for additional treatment steps. Balancing adsorbent dosage ensures cost-effective operation. Experiments were done using a RB-5 solution with an initial concentration of 500 mg L^{-1}. Fig. 3 shows that the percentage of removal increases as the adsorbent dosage increases; however, the dye adsorption capacity (q) is reduced. At 0.25 g L^{-1}, the q is approximately 1113 mg g^{-1} (55 %-removal) for the LR-Control biochar, 1234 mg g^{-1} (62 %-removal) for the LR-Boron biochar, and 1323 mg g^{-1} (66 %-removal) for the LR-Sulfur biochar.

Table 2
Surface elemental composition according to XPS analysis (values given in at%).

		LR-Control	LR-Boron	LR-Sulfur
C	C-C	64.11	71.01	61.03
	C=O	6.51	5.32	5.41
	C-O	18.21	12.39	16.4
	COO	3.96	3.31	4.29
	π-π	4.25	5.88	3.61
O	C-O-	1.51	1.08	0.68
	C=O	1.01	0.46	3.08
	OH-			0.28
	π-π	0.44	0.3	
B	B_2O_3		0.25	
S	C-S-C			3.3
	R-S(=O)-R′			1.92
C/O		32.8	53.2	22.4

When the dosage is increased to 0.5 g L^{-1}, the percentage of dye removal approaches 92–95 % depending on the biochar, but the adsorption capacity (q) is reduced to 920 mg g^{-1} (LR-Contol), 932 mg g^{-1} (LR-Boron), and 948 mg g^{-1} (LR-Sulfur). Beyond this adsorbent dose, the q continues to drop, and the percentage of removal reaches 100 %. Therefore, 0.5 g biochar L^{-1} was chosen for kinetic and isotherm studies described in the following sections. This sample dosage helps to reduce the overuse of adsorbent, which leads to excessive waste generation.

3.2.3. Reactive black-5 kinetic of adsorption

Measuring the kinetics of the adsorption of contaminants from water is crucial for understanding adsorption efficiency. Kinetic measurements provide insight into how quickly contaminants are removed from water and help to assess the efficiency of activated biochar as an adsorbent. Fig. 4 shows the kinetic measurements done at room temperature (296 K) for the LR-Control, LR-Boron, and LR-Sulfur biochars using RB-5 solution with an initial concentration of 500 and 1000 mg L^{-1} and contact times between 1 and 600 min. The kinetic profile shows a typical pattern where the q increases with time. This increase is rapid during the first stage when the adsorption sites are unoccupied and slows down gradually as equilibrium approaches. With the initial dye concentrations used here, equilibrium is reached in approximately 300 min.

The measurements were evaluated using the nonlinear pseudo-first-order (PFO), pseudo-second-order (PSO), and Avrami fractional order (AFO) kinetic models (equations are shown in the supplementary materials). The kinetic parameters are depicted in Table 3. The quality of the fitting was judged based on the adjusted determination coefficient (R^2_{adj}) and the standard deviation of residues (SD) [43–46]; equations are shown in the supplementary materials. The lower the standard residual deviation (SD) and R^2_{adj} values closer to 1, the minor the difference between predicted and measured kinetic data are obtained. According to the results, the kinetics of adsorption of RB-5 onto the studied biochars align with the AFO model. The Avrami kinetic model equation features the Avrami exponent (n_{Av}), a fractional number that signifies possible variations in the adsorption mechanism during the adsorption process. As a result, the adsorption mechanism can adhere to multiple kinetic orders that change as the adsorbate interacts with the adsorbent. Besides, the increase in the initial concentration of the dye caused an increase in the equilibrium constants (k_1, k_2, and k_{AV}), meaning a fast adsorption process controlled by the concentration gradient.

In order to simplify the understanding of the results from the kinetic measurements, the initial sorption rate (***ho***) depicted in Eq. 1 [47] was calculated for the AFO model, i.e., the most suitable model.

$$h_O = k_{AV}.q_{AV} \quad (1)$$

where, ***ho*** denotes the initial sorption rate (mg g^{-1} min^{-1}), $\boldsymbol{k_{AV}}$ is the rate constant (min^{-1}), and $\boldsymbol{q_{AV}}$ is the amount adsorbed at equilibrium (mg g^{-1}).

Comparing the h_o values for the AFO model (Table 3) at the same initial dye concentration, one can see that the values for the LR-Boron and LR-Sulfur biochars are higher than that of the LR-control, meaning that the treatment with boron and sulfur improved the adsorption kinetics, i.e., these two carbons are more efficient. The LR-Sulfur biochar presented the lowest specific surface area (Fig. 1) and the highest h_o values compared to the other two. This confirms that adding B and S during biochar production leads to structural and chemical changes in the surface of the adsorbent that facilitate the uptake of RB-5.

3.2.4. Reactive black-5 adsorption equilibrium isotherms

The measurement of equilibrium adsorption isotherms is a crucial aspect of characterizing activated biochar, and it helps gain detailed insights into the adsorption capacities and mechanisms of adsorption, which directly influence its performance and efficiency in these applications. These models help quantify the maximum adsorption capacity

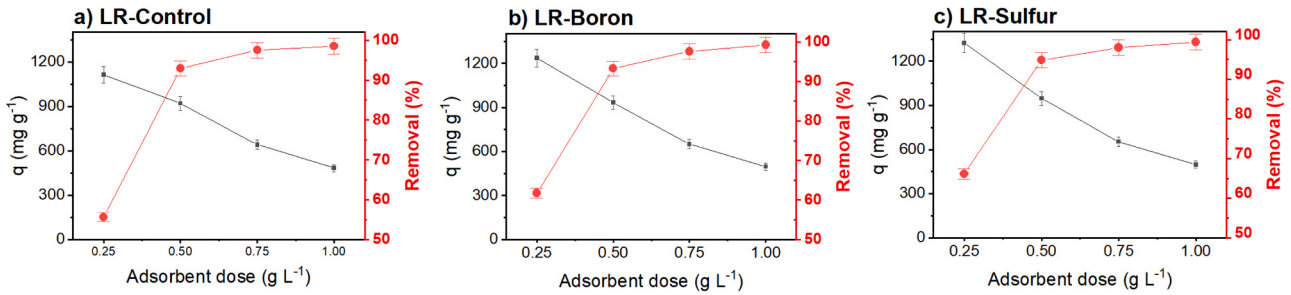

Fig. 3. The influence of adsorbent dosage on the sorption capacity and in the percentage of removal of reactive black-5 for the logging residues-based biochars. Temperature = 296 K, pH = 6, $[RB\text{-}5]_0$ = 500 mgL^{-1}.

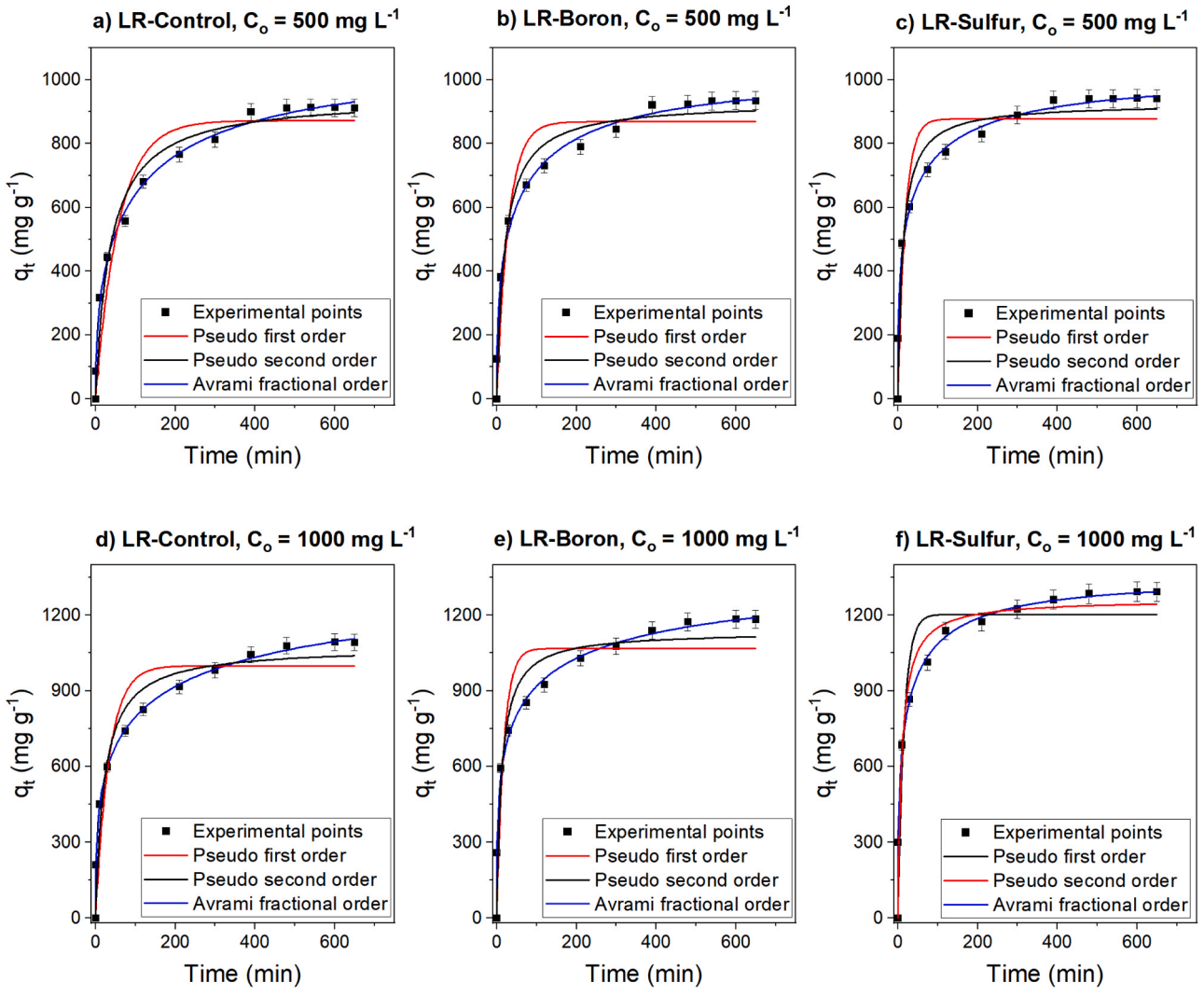

Fig. 4. Kinetic of adsorption of reactive black-5 onto the biochars. Adsorbent dosage = 0.5 g L^{-1}, initial pH = 6.0, temperature = 296 K, $[RB\text{-}5]_0$= 500 mg L^{-1} (a, b, c) and 1000 mg L^{-1} (d, e, f).

and describe how adsorption varies with the adsorbate concentration, which is critical for designing and optimizing adsorption systems [44–46].

Equilibrium isotherms were measured at 296 K, 306 K, and 316 K. The Langmuir, Freundlich, and Liu nonlinear models were used for evaluation, and the equation for each model is shown in the supplementary materials. The results from the fitting of the experimental measurements are shown in Fig. 5. The Freundlich isotherm model is based on the fact that adsorption takes place in multiple layers on the adsorbent's surface without reaching saturation and that the energy at each active site varies. In contrast, the Langmuir model assumes monolayer adsorption and admits that all active sites present the same energy. Liu's model integrates elements from both the Freundlich and Langmuir models [48]. It accounts for the saturation of the adsorbent but with multiple adsorption layers and active sites with different energy levels.

The parameters obtained from the nonlinear regression are shown in Table 4. The suitability of the models to describe the experimentally

Table 3
Kinetic parameters of reactive black-5 adsorption on the biochars.

C_0 (mg L^{-1})	500 LR-Control	1000	500 LR-Boron	1000	500 LR-Sulfur	1000
PFO						
q_1 (mg g^{-1})	872.2	999.1	868.7	1068	878.1	1203
k_1 (min^{-1})	0.017	0.029	0.034	0.056	0.055	0.064
R^2_{adj}	0.936	0.891	0.925	0.881	0.906	0.915
SD (mg g^{-1})	82.73	121.2	87.44	133.9	94.66	124.3
PSO						
q_2 (mg g^{-1})	948.1	1074	930.6	1135	925.7	1262
k_2 (g mg^{-1} min^{-1})	2.871×10^{-5}	4.232×10^{-5}	5.375×10^{-5}	7.086×10^{-5}	8.047×10^{-5}	8.947×10^{-5}
R^2_{adj}	0.973	0.949	0.973	0.943	0.961	0.965
SD (mg g^{-1})	53.46	82.65	52.48	92.34	61.13	79.98
AFO						
q_{AV} (mg g^{-1})	920.6	1149	942.5	1258	958.9	1333
k_{AV} (min^{-1})	0.019	0.064	0.033	0.085	0.049	0.098
n_{AV}	0.469	0.354	0.431	0.332	0.381	0.374
R^2_{adj}	0.996	0.999	0.995	0.996	0.996	0.998
h_o (mg g^{-1} min^{-1})	17.49	73.54	31.10	106.9	46.99	130.6
SD (mg g^{-1})	21.27	10.71	21.63	23.61	19.73	17.84

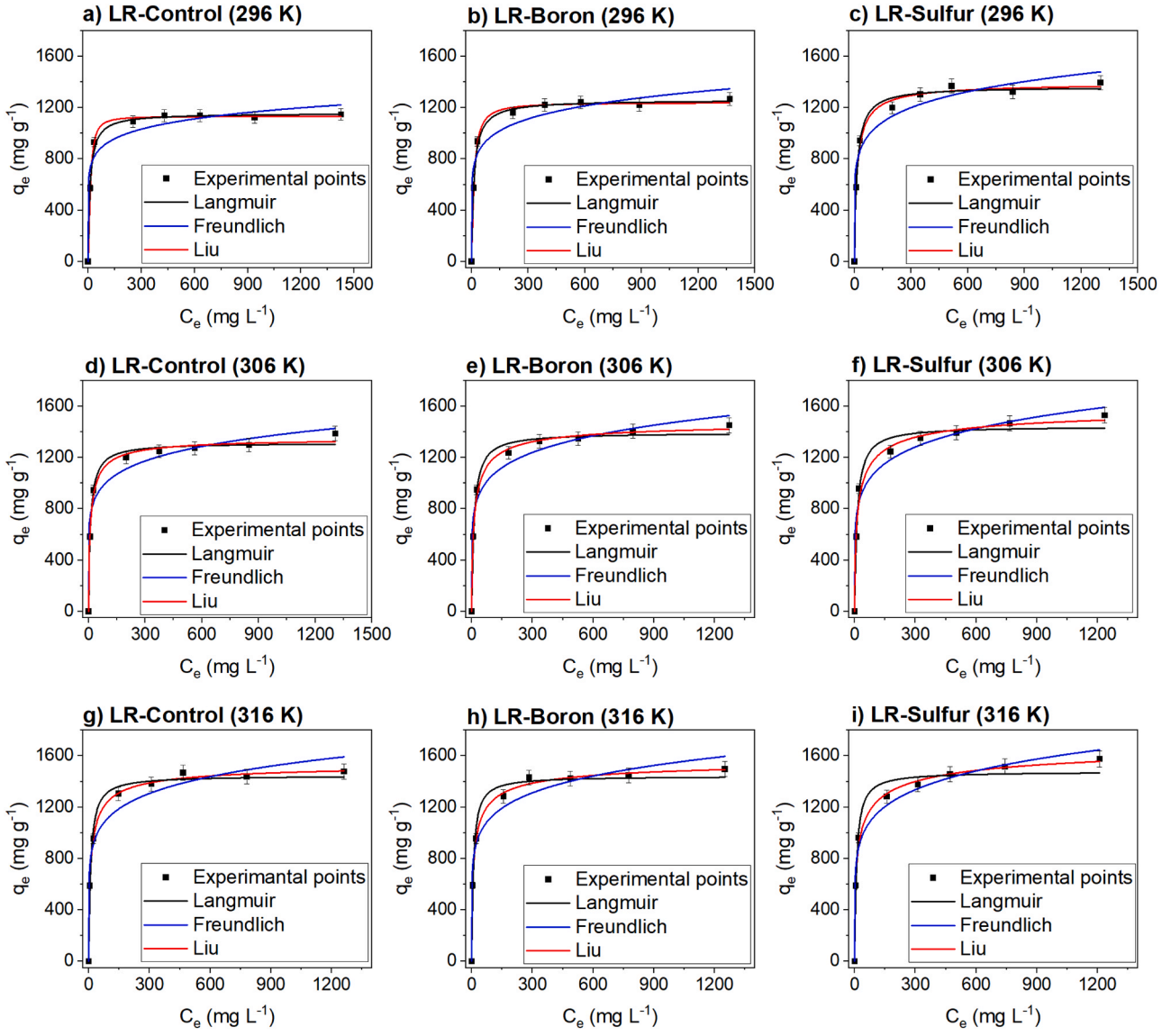

Fig. 5. Isotherms of adsorption of reactive black-5 onto the biochars at different temperatures. Conditions: adsorbent dosage = 0.5 g L^{-1}, pH = 6.0, temperature = 296 K (a, b, c), 306 K (d, e, f), and 316 K (g, h, i).

Table 4
Equilibrium parameters of reactive black-5 adsorption on LR-Control, LR-Boron, and LR-Sulfur biochars.

T (K)	296	306	316
	LR-Control		
Langmuir			
q_{max} (mg g^{-1})	1156	1314	1446
K_L (L mg^{-1})	0.087	0.093	0.108
R^2_{adj}	0.993	0.992	0.988
SD (mg g^{-1})	33.83	41.53	56.66
Freundlich			
K_F ((mg g^{-1}) (mg $L^{-1})^{-1/n}_F$)	557.5	548.6	596.6
n_F	9.262	7.506	7.274
R^2_{adj}	0.943	0.968	0.961
SD (mg g^{-1})	97.74	85.43	106.1
Liu			
q_{max} (mg g^{-1})	1132	1356	1419
K_g(L mg^{-1})	0.078	0.091	0.094
n_L	1.537	0.776	0.651
R^2_{adj}	0.998	0.993	0.998
SD (mg g^{-1})	16.94	40.41	22.31
	LR-Boron		
Langmuir			
q_{max} (mg g^{-1})	1260	1394	1482
K_L (L mg^{-1})	0.075	0.085	0.121
R^2_{adj}	0.996	0.992	0.982
SD (mg g^{-1})	28.32	46.07	70.75
Freundlich			
K_F ((mg g^{-1}) (mg $L^{-1})^{-1/n}_F$)	542.2	544.6	600.2
n_F	7.939	6.936	7.294
R^2_{adj}	0.949	0.971	0.966
SD (mg g^{-1})	101.5	87.44	98.31
Liu			
q_{max} (mg g^{-1})	1240	1488	1586
K_g(L mg^{-1})	0.073	0.078	0.093
n_L	1.242	0.671	0.583
R^2_{adj}	0.997	0.996	0.997
SD (mg g^{-1})	25.48	32.24	26.97
	LR-Sulfur		
Langmuir			
q_{max} (mg g^{-1})	1363	1445	1497
K_L (L mg^{-1})	0.073	0.084	0.111
R^2_{adj}	0.993	0.985	0.978
SD (mg g^{-1})	41.49	66.09	81.47
Freundlich			
K_F ((mg g^{-1}) (mg $L^{-1})^{-1/n}_F$)	533.2	536.8	569.3
n_F	7.031	6.551	6.685
R^2_{adj}	0.959	0.973	0.981
SD (mg g^{-1})	99.98	86.51	75.38
Liu			
q_{max} (mg g^{-1})	1396	1617	1766
K_g(L mg^{-1})	0.057	0.059	0.071
n_L	0.832	0.573	0.472
R^2_{adj}	0.994	0.988	0.996
SD (mg g^{-1})	40.31	56.36	34.85

measured points was judged based on the R^2_{adj} and SD values. The results showed that the Liu isotherm model was the most adequate to describe the experimental measurements because resulted in the highest R^2_{adj} and lowest SD, suggesting that the q predicted by this model is closest to the values measured experimentally. The highest Q_{max} were obtained at 316 K, and according to the Liu model, are 1419 mg g^{-1} (LR-Control), 1586 mg g^{-1} (LR-Boron), and 1766 mg g^{-1} (LR-Sulfur), demonstrating the efficacy of the sulfur treatment.

3.2.5. *Reactive Black-5 adsorption performance of the produced biochars, comparison with other types of adsorbents from the literature*

The kinetic and isotherm studies showed that the adsorbents produced in this work presented a remarkable efficiency for removing RB-5 dye from aqueous solutions. Although the comparison of adsorbents of different natures is difficult because each adsorbent has its own merits and demerits, here is a comparison of Q_{max} values of different adsorbents obtained from the literature (Table 5). For an easy comparison, we assume that the Q_{max} values in Table 5 were obtained at optimum conditions. Thus, it can be seen that the adsorption efficiency of the three LR-carbons was higher compared to the other adsorbents shown in Table 5, which could be attributed to their well-developed porosity and high surface areas as well as the presence of surface functional groups. Therefore, considering the extremely high Q_{max} of the logging residues-based carbons developed in this work, it can be safely stated that they can be considered highly effective adsorbents for removing pollutants from polluted waters.

3.2.6. *Thermodynamic study*

The thermodynamic parameters of adsorption, ΔH°, and ΔS°, determined using the nonlinear van't Hoff plot, are shown in Table 6. These values were derived from the K_g values obtained from the Liu isotherm at temperatures ranging from 296 to 316 K (Table 4) [54]. The standard Gibb's energy change (ΔG°) values were all negative within this temperature range, meaning that the adsorption process was favorable and spontaneous for the three activated biochars. ΔS° is positive for the three adsorbents within this temperature range, meaning an adsorption process where the RB-5 molecules remained less ordered on

Table 6
Thermodynamic parameters of RB-5 on LR-Control, LR-Boron, and LR-Sulfur biochars.

T (K)	ΔG^0 (kJ mol^{-1})	ΔH^0 (kJ mol^{-1})	ΔS^0 (J mol^{-1} K^{-1})
LR-Control			
296	−27.69	6.32	115
306	−29.02		
316	−30.01		
LR-Boron			
296	−27.55		
306	−28.50	10.0	127
316	−30.04		
LR-Sulfur			
296	−26.93		
306	−27.96	8.68	120
316	−29.31		

Table 5
Tabulated comparison of Reactive Black-5 adsorption capacity and other process parameters obtained from different adsorbents reported in the literature.

Adsorbent	SSA_{BET} (m^2/g)	Temperature (°C)	Isotherm	Q_{max} (mg/g)	Ref.
Powder activated carbon	900	20	Langmuir	58.823	[49]
Fly ash	3.55	20	Langmuir	7.936	[49]
Polyacrylamide/silica nanoporous composite	20.78	25	Langmuir	454.54	[50]
Acid-treated brow algae (*Laminaria* sp.) biosorbent	n.d.	40	Langmuir	101.5	[51]
Commercial activated carbon (F400)	793	n.d.	Langmuir	175.8	[52]
Bone char	107	n.d.	Langmuir	156.5	[52]
Bamboo H_3PO_4 activated carbon (1:2)	2123	n.d.	Langmuir	446.98	[52]
Bamboo H_3PO_4 activated carbon (1:6)	1400	n.d.	Langmuir	545.22	[52]
Cetyltrimethylammonium bromide modified zeolite	n.d.	30	Langmuir	12.93	[53]
Logging residue (LR-Control)	3141	43	Liu	1419	This work
Logging residue LR-Boron	2645	43	Liu	1586	This work
Logging residue LR-Sulfur	2524	43	Liu	1766	This work

the solid-liquid interface. The adsorption process was found to be endothermic with ΔH° values of 6.32 kJ mol^{-1} for LR-Control, 10.0 kJ mol^{-1} for LR-Boron, and 8.68 kJ mol^{-1} for LR-Sulfur biochar. These values of ΔH° (lower than 40 kJ mol^{-1}) indicate that the adsorption process is physical in nature, involving hydrogen bonding, n-π interaction, π-π stacking, and van der Walls interactions [55,56].

3.2.7. Adsorption mechanism

Based on the physicochemical characterization data of the LR-carbon materials as well as the literature data, an overall mechanism of adsorption can be proposed. Due to the fact that all three LR-carbon adsorbents presented a very high porosity, pore filling should be the primary adsorption mechanism of RB-5 [22,46]. For instance, the molecule size of RB-5 is about 2.301 nm [57], which it can easily be adsorbed by pores in the range of mesoporosity. Interestingly, the number of mesopores about 4.0 nm is much higher in LR-sulfur, followed by LR-Boron and LR-Control, respectively, and the adsorption of RB-5 followed the same order (LR-sulfur>LR-Boron>LR-Control). The presence of mesopores with a size higher than 2.301 nm (that is the size of the RB-5) facilitates the dye molecule diffusion.

Besides pore filling, the surface functional groups also have influenced the RB-5 molecules through electrostatic interaction, hydrogen bonding, π-π interaction, and Lewis acid-base interactions as illustrated in Fig. 6. For instance, hydrogen bonding between H of the RB-5 and O, H, and S-atoms present in LR-biochars should take place (see Fig. S5, supplementary material). The π-π interaction takes place between the aromatic rings of LR-carbons and aromatic rings of RB-5 molecules. LR-sulfur has thiophene (C-S-C) that can create a strong electron-donating effect (creating a positive effect) towards the sulfonate groups of RB-5 (that are negatively charged) through electrostatic interactions [57]. Besides, these two sulfonate groups are negatively charged even in highly acid conditions, due to their pK_a values that are lower than zero [57], and the pH_{PZC} of the carbons are 4.94, 6.52, and 7.94 for LR-Control, LR-Boron, and LR-Sulfur, respectively; which means their surfaces are positively charged, which can easily attract RB-5 molecules via electrostatic interactions [22,46].

Thus, it is worthwhile to state that the main mechanisms involved in the adsorption of RB-5 on the LR-carbons are pore-filling, electrostatic attraction, hydrogen bonding, and π-π EDA interactions (Fig. 6).

3.2.8. Treatment of dye synthetic effluents

As shown in previous sections, the three biochars showed outstanding efficiency in removing only RB-5 from aqueous solutions. Two aqueous dye-based synthetic effluents of different concentrations (Table 1) were used to test the adsorbents in more realistic conditions using adsorbent dosages of 0.5 and 1 g L^{-1} at a temperature of 296 K. The results in Fig. 7 demonstrate that the three biochars are highly efficient in removing contaminants from complex mixtures. The integrated area under the UV-Vis spectra was used to measure the percentage of removal. The results show that the biochars treated with boron and sulfur were more effective, following previous results using a single dye. Note that the untreated effluents were diluted 10 times before taking the UV-Vis spectra, and the treated effluents were not diluted. An adsorbent dosage of 0.5 g L^{-1} was enough to remove between 94 % and 97 % of the dyes from effluent-1 (less concentrated) and between 80 % and 84 % of the dyes from effluent-2 (more concentrated). Increasing the sample dosage to 1 g L^{-1} led to a percentage of removal near 100 % for effluent-1 and 88–96 % for effluent-2. This means using a sample dosage of 1 g L^{-1} to treat effluent-1 can be considered unnecessary because the adsorbent was not saturated, i.e., still can remove more contaminants than what was available in the effluent.

3.2.9. Regeneration of spent adsorbents

A total of seven adsorption-desorption/regeneration cycles were done for each carbon. The results from the regeneration, shown in Fig. 8, indicate that the percentage of removal of the RB-5 from the solution decreased with cycling, but both the LR-Boron and LR-Sulfur were more stable compared to the LR-Control biochar. The loss of performance that occurs with the cycling of the LR-Control biochar may be attributed to mechanical degradation of the microporous matrix, or dye molecules that get sized in small pores. The other two biochars present a higher amount of mesopores that are probably less susceptible to mechanical damage, and adsorbed dye molecules can probably be desorbed easily compared to the control sample. The higher amount of active adsorption sites in the LR-Sulfur may have also contributed to higher cyclability.

4. Conclusions

In this work, three highly different porous carbon materials were prepared using pine logging residues as a carbon precursor. Boron and sulfur were utilized as chemical modifiers, and KOH as a chemical activator. The prepared materials exhibited extremely high surface areas (2524–3141 m^2 g^{-1}). The sample treated with boron (LR-Boron) showed

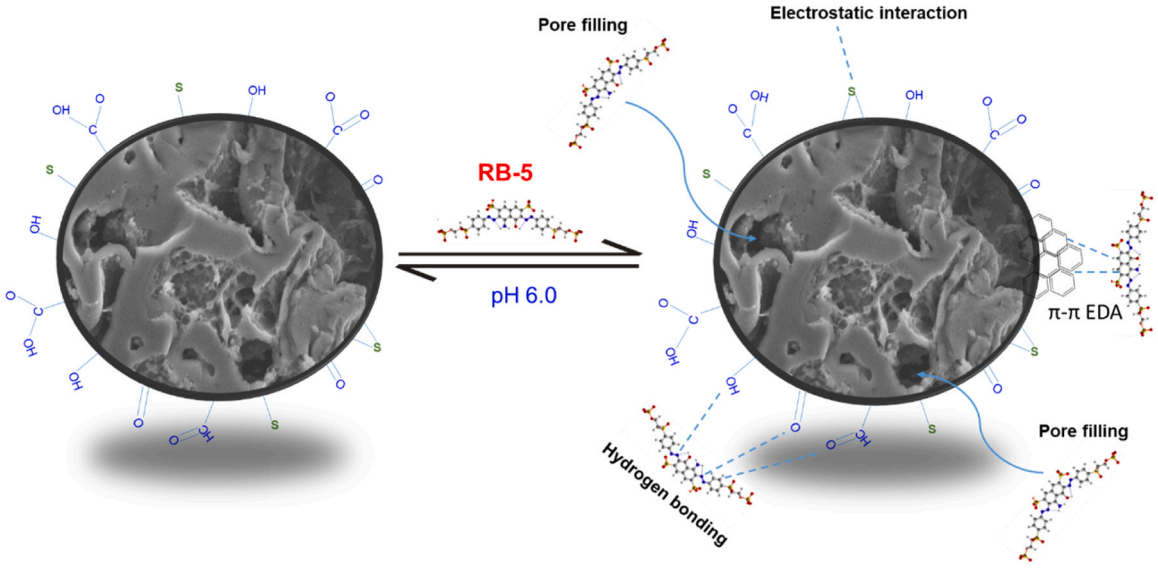

Fig. 6. Suggested adsorption mechanism involving LR-carbons and RB-5 dye.

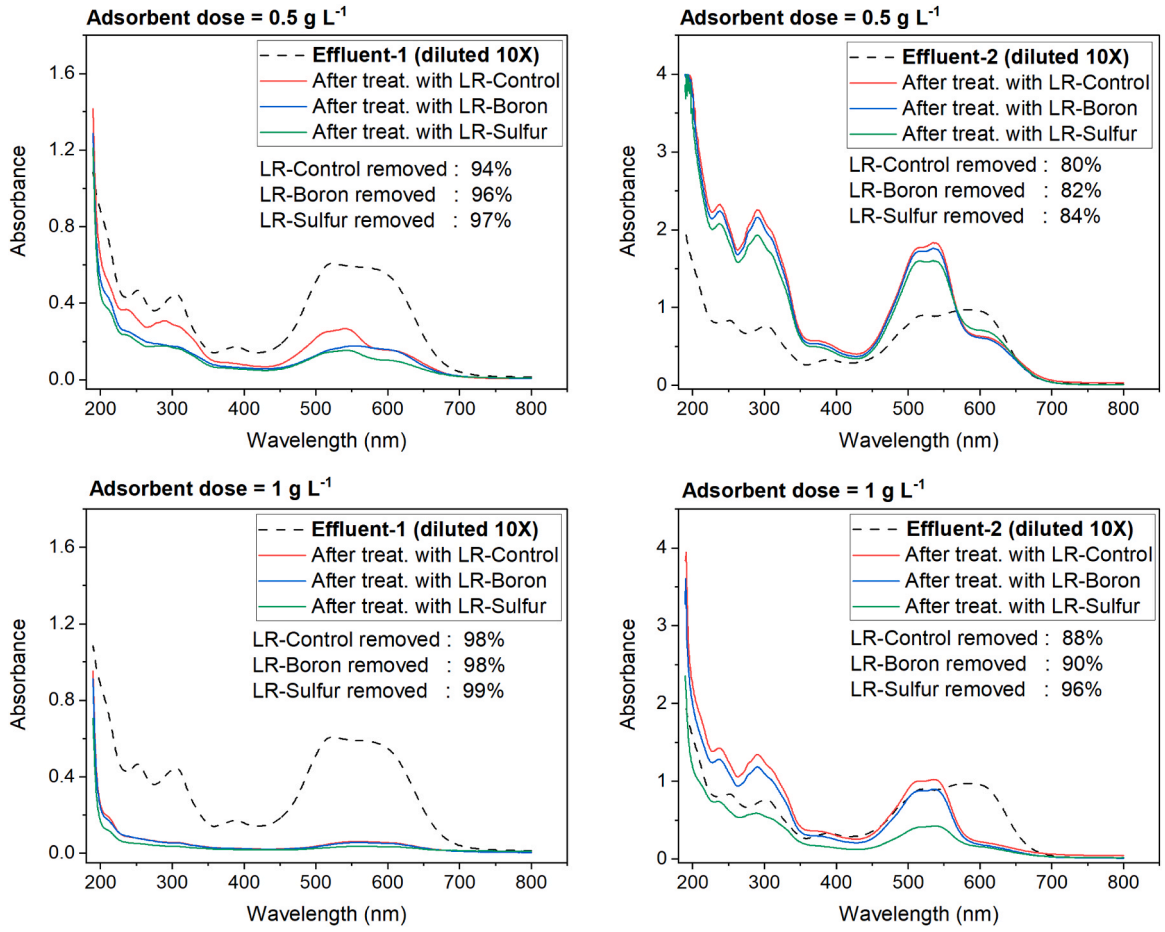

Fig. 7. Removal of dyes from synthetic effluents. Note that the dilution factor for the raw effluents is 10, and the effluent after treatment with the carbons was not diluted.

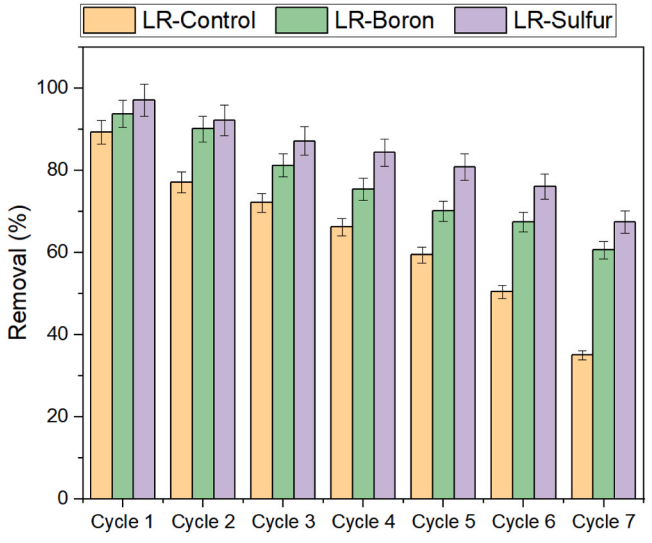

Fig. 8. Regeneration of the biochars. Conditions: Temperature = 296 K, RB-5 dye concentration = 1000 mg L^{-1}.

an exceptional degree of graphitization of (I_D/I_G=0.45), compared to the sulfur treated (LR-Sulfur, I_D/I_G=1.02) and the control sample (LR-control, without boron or sulfur, I_D/I_G=0.81). The three carbons were tested as adsorbents for the removal of reactive black-5 (RB-5) and synthetic effluents containing several dyes. The kinetic studies indicated that sulfur-treated carbon displayed the fastest kinetics because of the higher mesoporosity and amount of adsorption active sites incorporated in the carbon lattice by the sulfur atoms. All three carbons exhibited outstanding adsorptive capacities with Q_{max} 1419 mg g^{-1} (LR-Control), 1586 mg g^{-1} (LR-Boron), and 1766 mg g^{-1} (LR-Sulfur) at 316 K according to the best-fitted isotherm model (Liu model). These removal performances were higher than most RB-5 adsorption capacities reported in the literature for different types of adsorbents. The efficient adsorptive performance of the prepared carbons could be due to the multiple adsorption mechanisms such as pore filling, electrostatic interactions, surface complexation, hydrogen interaction, and π-π interaction. Thermodynamic studies showed that the adsorption process was endothermic, favorable, spontaneous, and physical in nature. When tested for removal of a mix of different dyes in synthetic aqueous effluents, all carbons exhibited outstanding performance, suggesting their excellent applicability in treating real effluents. Depending on the effluent composition, the removal percentages of dyes from effluents were up to 99 % when using adsorbent dosages of 0.5–1 g L^{-1}. The LR-Boron and LR-Sulfur demonstrated to have better cyclability, keeping a percentage of removal of approximately 60–67 % after 7 regeneration cycles compared to 35 % for the LR-control biochar. Due to their high porosity and composition, the carbons produced here could also be used in applications such as the construction of electrodes for electrochemical storage devices, e.g., supercapacitors and batteries.

5. Challenges and research directions

Heteroatom doping (e.g., nitrogen, sulfur, phosphorus, boron, or oxygen) in carbon materials is a widely used strategy to improve their

physicochemical properties and boosting their adsorptive properties. However, despite the significant benefits the doping process brings, heteroatom doping faces several major challenges that need to be deeply addressed in future research for achieving an optimal performance. Here we present a few key challenges and research directions. (i) Precise control of doping degree and uniformity: achieving a uniform distribution of heteroatoms within the carbon matrix is difficult. Inconsistent doping can lead to uneven dopant distribution over the carbon surface, which reduces the possibility of achieving a maximum potential of adsorption performance. (ii) Optimization of doping concentration: understanding/determining the optimal concentration of heteroatoms is extremely important to obtain materials of optimized performance. A small amount of dopant may not significantly enhance properties, while excessive doping can disrupt the carbon structure and degrade performance. (iii) Synthesis methods: many heteroatom doping methods involve complex, multi-step processes that are time-consuming, energy-intensive, and costly. The optimization of the pyrolysis processes is crucial for obtaining materials with maximized properties/performances. (iv) Understanding the doping mechanism: the exact role of heteroatoms in changing the materials' physicochemical properties and enhancing adsorptive performance is not always fully understood. The interactions between heteroatoms and the carbon matrix can vary depending on the doping method and material structure, and more studies in this regard are crucial for better understanding how the doping process works regardless of the different types of dopant and biomass resources.

CRediT authorship contribution statement

Gentili Francesco G.: Writing – original draft, Supervision, Software, Methodology, Investigation, Formal analysis, Data curation, Conceptualization. **Mikkola Jyri-Pekka:** Writing – review & editing, Resources, Investigation. **Grimm Alejandro:** Writing – original draft, Visualization, Validation, Supervision, Project administration, Methodology, Investigation, Funding acquisition, Formal analysis, Data curation, Conceptualization. **Conrad Sarah:** Writing – review & editing, Visualization, Supervision, Resources, Investigation, Conceptualization. **Lima Eder Claudio:** Writing – original draft, Visualization, Methodology, Investigation, Formal analysis, Data curation. **dos Reis Glaydson Simoes:** Writing – original draft, Visualization, Supervision, Methodology, Investigation, Formal analysis, Data curation, Conceptualization. **Hu Tao:** Writing – review & editing, Software, Resources, Investigation, Data curation. **Lassi Ulla:** Writing – review & editing, Resources, Investigation, Data curation. **Silva Luis F.O:** Resources.

Declaration of Competing Interest

The authors declare that they have no known competing financial interests or personal relationships that could have appeared to influence the work reported in this paper.

Acknowledgments

Dr. Alejandro Grimm acknowledges financial support from EU/Interreg Aurora (Project: Nature Refines, grant No. 20361711), the Swedish Research Council FORMAS (grant No. 2021–00877), and Kempestiftelserna (grant No. JCSMK23-0145). The authors thank the Vibrational Spectroscopy Core Facility (ViSp), Chemical Biological Centre (KBC), and Umeå University for the Raman measurements. Dr. Glaydson dos Simoes Reis gratefully acknowledges financial support from the Research Council of Finland (Academy Research Fellows 2024, Project: Bio-Adsorb&Energy, grant No. 361583). This work is also a part of the activities of the Johan Gadolin Process Chemistry Centre at Åbo Akademi University in Finland as well as the Bio4Energy program in Sweden. Further, the Wallenberg Wood Science Center under auspices of the Knut and Alice Wallenberg Foundation is acknowledged. Dr. Silva thanks Fundação de Amparo à Pesquisa e Inovação do Estado de Santa Catarina (FAPESC), Edital 43/2024.

Appendix A. Supporting information

Supplementary data associated with this article can be found in the online version at doi:10.1016/j.colsurfa.2025.136486.

Data availability

Data will be made available on request.

References

[1] U. Shanker, M. Rani, V. Jassal, Degradation of hazardous organic dyes in water by nanomaterials, Environ. Chem. Lett. 15 (2017) 623–642, https://doi.org/10.1007/s10311-017-0650-2.
[2] M.F. Hanafi, N. Sapawe, A review on the water problem associate with organic pollutants derived from phenol, methyl orange, and remazol brilliant blue dyes, Mater. Today-Proc. 31 (2020) A141–A150, https://doi.org/10.1016/j.matpr.2021.01.258.
[3] K. Balakrishna, A. Rath, Y. Praveenkumarreddy, K.S. Guruge, B. Subedi, A review of the occurrence of pharmaceuticals and personal care products in Indian water bodies, Ecotox. Environ. Safe. 137 (2017) 113–120, https://doi.org/10.1016/j.ecoenv.2016.11.014.
[4] J. Wang, S. Wang, Removal of pharmaceuticals and personal care products (PPCPs) from wastewater: a review, J. Environ. Manag. 182 (2016) 620–640, https://doi.org/10.1016/j.jenvman.2016.07.049.
[5] Y. Zhao, F. Liu, M. Yang, K. Qi, A. Zada, J. Pan, Removal of bisphenol A (BPA) from aqueous solution by potassium carbonate modified wetland plant biochars, Colloid Surf. A 703 (2024) 135184, https://doi.org/10.1016/j.colsurfa.2024.135184.
[6] Y. Zhao, M. Yang, K. Qi, J. Pan, The adsorption of bisphenol A by biochars modified with potassium phosphate, Desalin. Water Treat. 319 (2024) 100444, https://doi.org/10.1016/j.dwt.2024.100444.
[7] Y. Zhao, M. Yang, K. Qi, A. Peng, J. Pan, Hydrogen peroxide-modified biochars from wetland plants for bisphenol A removal in water, Ind. Eng. Chem. Res. 63 (2024) 13389–13400, https://doi.org/10.1021/acs.iecr.4c01179.
[8] M.P. Ormad, N. Miguel, A. Claver, J.M. Matesanz, J.L. Ovelleiro, Pesticides removal in the process of drinking water production, Chemosphere 71 (2008) 97–106, https://doi.org/10.1016/j.chemosphere.2007.10.006.
[9] A.S. Jatoi, Z. Hashmi, R. Adriyani, A. Yuniarto, S.A. Mazari, F. Akhter, N. M. Mubarak, Recent trends and future challenges of pesticide removal techniques–a comprehensive review, J. Environ. Chem. Eng. 9 (2021) 105571, https://doi.org/10.1016/j.jece.2021.105571.
[10] A.A. Akinpelu, M.E. Ali, M.R. Johan, R. Saidur, M.A. Qurban, T.A. Saleh, Polycyclic aromatic hydrocarbons extraction and removal from wastewater by carbon nanotubes: a review of the current technologies, challenges and prospects, Process Saf. Environ. 122 (2019) 68–82, https://doi.org/10.1016/j.psep.2018.11.006.
[11] S. Sabir, Approach of cost-effective adsorbents for oil removal from oily water, Crit. Rev. Env. Sci. Tec. 45 (2015) 1916–1945, https://doi.org/10.1080/10643389.2014.1001143.
[12] N.A.A. Qasem, R.H. Mohammed, D.U. Lawal, Removal of heavy metal ions from wastewater: a comprehensive and critical review, npj Clean. Water 4 (2021) 36, https://doi.org/10.1038/s41545-021-00127-0.
[13] C.F. Carolin, P.S. Kumar, A. Saravanan, G.J. Joshiba, M. Naushad, Efficient techniques for the removal of toxic heavy metals from aquatic environment: a review, J. Environ. Chem. Eng. 5 (2017) 2782–2799, https://doi.org/10.1016/j.jece.2017.05.029.
[14] M. Ismail, K. Akhtar, M.I. Khan, T. Kamal, M.A. Khan, A.M. Asiri, J. Seo, S.B. Khan, Pollution, toxicity, and carcinogenicity of organic dyes and their catalytic bio-remediation, Curr. Pharm. Des. 25 (2019) 3645–3663, https://doi.org/10.2174/1381612825666191021142026.
[15] A. Tkaczyk, K. Mitrowska, A. Posyniak, Synthetic organic dyes as contaminants of the aquatic environment and their implications for ecosystems: a review, Sci., Total Environ. 717 (2020) 137222, https://doi.org/10.1016/j.scitotenv.2020.137222.
[16] R. Rashid, I. Shafiq, P. Akhter, M.J. Iqbal, M. Hussain, A state-of-the-art review on wastewater treatment techniques: the effectiveness of adsorption method, Environ. Sci. Pollut. Res. 28 (2021) 9050–9066, https://doi.org/10.1007/s11356-021-12395-x.
[17] K.Y. Foo, B.H. Hameed, An overview of dye removal via activated carbon adsorption process, Desalin. Water Treat. 19 (2010) 255–274, https://doi.org/10.5004/dwt.2010.1214.
[18] A. Grimm, G.S. dos Reis, V.M. Dinh, S.H. Larsson, J.P. Mikkola, E.C. Lima, S. Xiong, Hardwood spent mushroom substrate–based activated biochar as a sustainable bioresource for the removal of emerging pollutants from wastewater, Biomass-.-. Conv. Bioref. 14 (2024) 2293–2309, https://doi.org/10.1007/s13399-022-02618-7.
[19] N.L. Panwar, A. Pawar, Influence of activation conditions on the physicochemical properties of activated biochar: a review, Biomass-.-. Conv. Bioref. 12 (2020) 925–947, https://doi.org/10.1007/s13399-020-00870-3.
[20] H. Zeghioud, L. Fryda, H. Djelal, A. Assadi, A. Kane, A comprehensive review of biochar in the removal of organic pollutants from wastewater: characterization,

toxicity, activation/functionalization and influencing treatment factors, J. Water Process Eng. 47 (2022) 102801, https://doi.org/10.1016/j.jwpe.2022.102801.
[21] A. Grimm, G.S. dos Reis, S.G. Khokarale, S. Ekman, E.C. Lima, S. Xiong, M. Hultberg, Shiitake spent mushroom substrate as a sustainable feedstock for developing highly efficient nitrogen-doped biochars for the treatment of dye-contaminated water, J. Water Process Eng. 56 (2023) 104435, https://doi.org/10.1016/j.jwpe.2023.104435.
[22] G.S. dos Reis, J. Thivet, E. Laisné, V. Srivastava, A. Grimm, E.C. Lima, D. Bergna, T. Hu, U. Lassi, Synthesis of novel mesoporous selenium-doped biochar with high-performance sodium diclofenac and reactive orange 16 dye removals, Chem. Eng. Sci. 281 (2023) 119129, https://doi.org/10.1016/j.ces.2023.119129.
[23] S. Vigneshwaran, P. Sirajudheen, P. Karthikeyan, S. Meenakshi, Fabrication of sulfur-doped biochar derived from tapioca peel waste with superior adsorption performance for the removal of Malachite green and Rhodamine B dyes, Surf. Interfaces 23 (2021) 100920, https://doi.org/10.1016/j.surfin.2020.100920.
[24] S. Xue, J. Tan, X. Ma, Y. Xu, R. Wan, H. Tao, Boron-doped activated carbon derived from Zoysia sinica for Rhodamine B adsorption: the crucial roles of defect structures, FlatChem 34 (2022) 100390, https://doi.org/10.1016/j.flatc.2022.100390.
[25] L. Xu, Y. Qi, S. He, C. Wang, X. Jin, Q. Wang, K. Wang, P. Jin, Facile synthesis of boron-doped porous biochar as a metal-free adsorbent for efficient removal of aqueous tetracycline antibiotics, J. Environ. Sci. 152 (2025) 235–247, https://doi.org/10.1016/j.jes.2024.04.044.
[26] C. Chen, L.L. Zhou, Y.N. Huang, W.K. Wang, J. Xu, Boron regulates catalytic sites of biochar to enhance the formation of a surface-confined complex for improved peroxydisulfate activation, Chemosphere 301 (2022) 134690, https://doi.org/10.1016/j.chemosphere.2022.134690.
[27] W. Tian, H. Zhang, X. Duan, H. Sun, G. Shao, S. Wang, Porous carbons: structure-oriented design and versatile applications, Adv. Funct. Mater. 30 (2020) 1909265, https://doi.org/10.1002/adfm.201909265.
[28] L. Leng, R. Liu, S. Xu, B.A. Mohamed, Z. Yang, Y. Hu, J. Chen, S. Zhao, Z. Wu, H. Peng, H. Li, H. Li, An overview of sulfur-functional groups in biochar from pyrolysis of biomass, J. Environ. Chem. Eng. 10 (2022) 107185, https://doi.org/10.1016/j.jece.2022.107185.
[29] G. S. Dos Reis, A. Grimm, D.A. Fungaro, T. Hu, I.A. de Brum, E.C. Lima, M. Naushad, G.L. Dotto, U. Lassi, Synthesis of sustainable mesoporous sulfur-doped biobased carbon with superior performance sodium diclofenac removal: kinetic, equilibrium, thermodynamic and mechanism, Environ. Res. 251 (2024) 118595, https://doi.org/10.1016/j.envres.2024.118595.
[30] Q. Fan, C. Song, P. Fu, Advances in the improvement of the quality and efficiency of biomass-derived porous carbon: a comprehensive review on synthesis strategies and heteroatom doping effects, J. Clean. Prod. 452 (2024) 142169, https://doi.org/10.1016/j.jclepro.2024.142169.
[31] Z. Yang, Y. Xu, X. Sun, C. Nie, M. Chen, Q. Zhang, G. Luo, Induced synthesis of SO2-promoting and H2O-tolerant sorbents for elemental mercury removal from flue gas, Fuel 357 (2024) 29881, https://doi.org/10.1016/j.fuel.2023.129881.
[32] T. Yrjölä, Forest management guidelines and practices in Finland, Sweden and Norway, 11, European Forest Institute, Sweden and Norway, 2002. ⟨https://efi.int/sites/default/files/files/publication-bank/2018/ir_11.pdf⟩.
[33] E.L. Lindholm, J. Stendahl, S. Berg, P.A. Hansson, Greenhouse gas balance of harvesting stumps and logging residues for energy in Sweden, Scand. J. For. Res. 26 (2011) 586–594, https://doi.org/10.1080/02827581.2011.615337.
[34] P. Börjesson, L. Gustavsson, L. Christersson, S. Linder, Future production and utilisation of biomass in Sweden: potentials and CO2 mitigation, Biomass-.-. Bioenerg. 13 (1997) 399–412, https://doi.org/10.1016/S0961-9534(97)00039-1.
[35] G.S. dos Reis, S.H. Larsson, M. Thyrel, M. Mathieu, P.N. Tung, Application of design of experiments (DoE) for optimised production of micro-and mesoporous Norway spruce bark-activated carbons, Biomass-.-. Conv. Bioref. 13 (2023) 10113–10131, https://doi.org/10.1007/s13399-021-01917-9.
[36] M. Pawlyta, J.-N. Rouzaud, S. Duber, Raman microspectroscopy characterisation of carbon blacks: spectral analysis and structural information, Carbon 84 (2015) 479–490, https://doi.org/10.1016/j.carbon.2014.12.030.
[37] V. Piergrossi, C. Fasolato, F. Capitani, G. Monteleone, G. Postorino, P. Gislon, Application of Raman spectroscopy in chemical investigation of impregnated activated carbon spent in hydrogen sulfide removal process, Int. J. Environ. Sci. Technol. 16 (2019) 227–1238, https://doi.org/10.1007/s13762-018-1756-1.
[38] F. Jiang, Y. Yao, B. Natarajan, T. Yang, H. Gao, Y. Xie, L. Wang, Y. Xu, J. Chen, L. Gilman, L. Cui, Hu, Ultrahigh-temperature conversion of biomass to highly conductive graphitic carbon, Carbon 144 (2019) 241–248, https://doi.org/10.1016/j.carbon.2018.12.030.
[39] N.A. Banek, D.T. Abele, K.R. McKenzie, M.J. Wagner, Sustainable conversion of lignocellulose to high-purity, highly crystalline flake potato graphite, ACS Sustain. Chem. Eng. 6 (2018) 13199–13207, https://doi.org/10.1021/acssuschemeng.8b02799.
[40] Z. Yang, Z. Yao, G. Li, G. Fang, H. Nie, Z. Liu, X. Zhou, X. Chen, S. Huang, Sulfur-doped graphene as an efficient metal-free cathode catalyst for oxygen reduction, *ACS Nano* 6, 205–211, https://doi.org/10.1021/nn203393d.
[41] N.F. Cardoso, E.C. Lima, T. Calvete, I.S. Pinto, C.V. Amavisca, T.H. Fernandes, R. V. Pinto, W.S. Alencar, Application of aqai stalks as biosorbents for the removal of the dyes Reactive Black 5 and Reactive Orange 16 from aqueous solution, J. Chem. Eng. Data 56 (2011) 1857–1868, https://doi.org/10.1021/je100866c.
[42] J.E. Aguiar, B.T.C. Bezerra, A.C.A. Siqueira, D. Barrera, K. Sapag, D.C.S. Azevedo, S.M.P. Lucena, I.J. Silva, Jr, Improvement in the adsorption of anionic and cationic dyes from aqueous solutions: a comparative study using aluminium pillared clays and activated carbon, Separ. Sci. Technol. 49 (2014) 741–751, https://doi.org/10.1080/01496395.2013.862720.
[43] A. Bonilla-Petriciolet, D.I. Mendoza-Castillo, H.E. Reynel-Ávila (Eds.), Adsorption processes for water treatment and purification, 256, Springer, Berlin, 2017, https://doi.org/10.1007/978-3-319-58136-1.
[44] R.F. Pinheiro, A. Grimm, M.L.S. Oliveira, J. Vieillard, L.F.O. Silva, I.A.S. De Brum, E.C. Lima, M. Naushad, L. Sellaoui, G.L. Dotto, G.S. dos Reis, Adsorptive behavior of the rare earth elements Ce and La on a soybean pod derived activated carbon: application in synthetic solutions, real leachate and mechanistic insights by statistical physics modeling, Chem. Eng. J. 471 (2023) 144484, https://doi.org/10.1016/j.cej.2023.144484.
[45] G.S. dos Reis, G.L. Dotto, J. Vieillard, M.L.S. Oliveira, S.F. Lütke, A. Grimm, L.F. O. Silva, E.C. Lima, M. Naushad, U. Lassi, Nickel-aluminium layered double hydroxide as an efficient adsorbent to selectively recover praseodymium and samarium from phosphogypsum leachate, J. Alloy. Compd. 960 (2023) 170530, https://doi.org/10.1016/j.jallcom.2023.170530.
[46] M. Gonzalez-Hourcade, G.S. dos Reis, A. Grimm, V.M. Dinh, E.C. Lima, S. H. Larsson, F.G. Gentili, Microalgae biomass as a sustainable precursor to produce nitrogen-doped biochar for efficient removal of emerging pollutants from aqueous media, J. Clean. Prod. 348 (2022) 131280, https://doi.org/10.1016/j.jclepro.2022.131280.
[47] Y.S. Ho, Review of second-order models for adsorption systems, J. Hazard Mater. 136 (2006) 681–689, https://doi.org/10.1016/j.jhazmat.2005.12.043.
[48] Y. Liu, H. Xu, S.F. Yang, J.H. Tay, A general model for biosorption of Cd2+ , Cu2+ , and Zn2+ by aerobic granules, J. Biotechnol. 102 (2003) 233–239, https://doi.org/10.1016/S0168-1656(03)00030-0.
[49] Z. Eren, F.N. Acar, Adsorption of Reactive Black 5 from an aqueous solution: equilibrium and kinetic studies, Desalination 194 (2006) 1–10, https://doi.org/10.1016/j.desal.2005.10.022.
[50] A. Nematollahzadeh, A. Shojaei, M. Karimi, Chemically modified organic/inorganic nanoporous composite particles for the adsorption of reactive black 5 from aqueous solution, React. Funct. Polym. 86 (2015) 7–15, https://doi.org/10.1016/j.reactfunctpolym.2014.11.001.
[51] K. Vijayaraghavan, Y.S. Yun, Biosorption of C.I. Reactive Black 5 from aqueous solution using acid-treated biomass of brown seaweed Laminaria sp, Dyes Pigments 76 (2008) 726–732, https://doi.org/10.1016/j.dyepig.2007.01.013.
[52] A.W.M. Ip, J.P. Barford, G. McKay, Reactive Black dye adsorption/desorption onto different adsorbents: effect of salt, surface chemistry, pore size and surface area, J. Colloid Interf. Sci. 337 (2009) 32–38, https://doi.org/10.1016/j.jcis.2009.05.015.
[53] D. Karadag, M. Turan, E. Akgul, S. Tok, A. Faki, Adsorption equilibrium and kinetics of reactive black 5 and reactive red 239 in aqueous solution onto surfactant-modified zeolite, J. Chem. Eng. Data 52 (2007) 1615–1620, https://doi.org/10.1021/je7000057.
[54] E.C. Lima, A. Hosseini-bandegharaei, J.C. Moreno-pirajan, I. Anastopoulos, A critical review of the estimation of the thermodynamic parameters on adsorption equilibria. Wrong use of equilibrium constant in the Vant Hoof equation for calculation of thermodynamic parameters of adsorption, J. Mol. Liq. 273 (2019) 425–434, https://doi.org/10.1016/j.molliq.2018.10.048.
[55] Y. Dehmani, Y. Bengamra, I. Aadnan, R. Oukhrib, B.El Ibrahimi, M.Ait El Had, R. Chahboun, A. Dehbi, Y. Brahmi, T. Lamhasni, A. Abdallaoui, G. Giacoman-Vallejos, A. Sadik, E.C. Lima, Efficient removal of malachite green dye onto nickel oxide-based adsorbent: experimental and theoretical approaches, Int. J. Environ. Sci. Technol. 21 (2024) 3037–3052, https://doi.org/10.1007/s13762-023-05153-8.
[56] J. Xie, M. Liu, M. He, Y. Liu, J. Li, F. Yu, Y. Lv, C. Lin, X. Ye, Ultra-efficient adsorption of diclofenac sodium on fish-scale biochar functionalized with H3PO4 via synergistic mechanisms, Environ. Pollut. 322 (2023) 121226 https://doi.org/10.1016/j. envpol.2023.121226.
[57] N.F. Cardoso, E.C. Lima, T. Calvete, I.S. Pinto, C.V. Amavisca, T.H.M. Fernandes, R. B. Pinto, W.S. Alencar, Application of aqai stalks as biosorbents for the removal of the dyes, Reactive Black 5 and reactive orange 16 from aqueous solution, J. Chem. Eng. Data 56 (2011), 1857–186.